

Generative Adversarial Networks for Spatio-Spectral Compression of Hyperspectral Images

Akshara Preethy Byju, *Member, IEEE*, Martin Hermann Paul Fuchs, Alisa Walda,
and Begüm Demir, *Senior Member, IEEE*

Abstract—Deep learning-based image compression methods have led to high rate-distortion performances compared to traditional codecs. Recently, Generative Adversarial Networks (GANs)-based compression models, e.g., High Fidelity Compression (HiFiC), have attracted great attention in the computer vision community. However, most of these works aim for spatial compression only and do not consider the spatio-spectral redundancies observed in hyperspectral images (HSIs). To address this problem, in this paper, we adapt the HiFiC spatial compression model to perform spatio-spectral compression of HSIs. To this end, we introduce two new models: i) HiFiC using Squeeze and Excitation (SE) blocks (denoted as HiFiC_{SE}); and ii) HiFiC with 3D convolutions (denoted as HiFiC_{3D}). We analyze the effectiveness of HiFiC_{SE} and HiFiC_{3D} in exploiting the spatio-spectral redundancies with channel attention and interdependency analysis. Experimental results show the efficacy of the proposed models in performing spatio-spectral compression and reconstruction at reduced bitrates and higher reconstruction quality when compared to JPEG 2000 and the standard HiFiC spatial compression model. The code of the proposed models is publicly available at <https://git.tu-berlin.de/rsim/HSI-SSC>.

Index Terms—Spatio-spectral image compression, generative adversarial networks, deep learning, hyperspectral images.

I. INTRODUCTION

ADVANCEMENTS in hyperspectral imaging technologies have led to a significant increase in the volume of hyperspectral data archives. Dense spectral information provided by hyperspectral imagery leads to a very high capability for the identification and discrimination of the materials in a given scene. However, the storage and transmission of such high volume data hinders the development of these fields. This necessitates the need for efficient compression techniques that encode the data into fewer bits with minimal loss of information.

Hyperspectral image compression has been a long studied area with various methods developed so far. Generally, they can be divided into two categories: i) traditional approaches; and ii) learning-based approaches. Traditional approaches mostly rely on transform coding. As an example, in [1]

HSIs are compressed by applying the JPEG 2000 [2] algorithm in combination with a principal component analysis (PCA) that is responsible for spectral decorrelation as well as spectral dimensionality reduction. Lim et. al [3] apply a three dimensional wavelet transform to compress the HSIs. Abousleman et al. [4] use differential pulse code modulation (DPCM) to spectrally decorrelate the data while a 2D discrete cosine transform (DCT) coding scheme is used for spatial decorrelation.

On the other hand, the current state of the art in learning-based hyperspectral image compression is formed by convolutional autoencoders (CAEs) [5]–[8] that reduce the dimensionality of the latent space by sequentially applying convolutions and downsampling operations. The 1D-CAE [5], [6] therefore stacks multiple 1D convolutions combined with two pooling layers and LeakyReLU activation functions and thus only compresses in the spectral dimension. The spectral signal compressor network (SSCNet) [7] incorporates spatial compression by utilizing 2D convolutions, PReLUs and 2D max poolings for encoding and strided 2D transposed convolutions for decoding. 3D-CAE [8] combines spatial and spectral compression. The network is built by strided 3D convolutions, LeakyReLU, 3D batch normalization, residual blocks and upsampling layers in the decoder. However, due to the fixed compression ratio of CAEs and their relatively high bitrates, there is a need for developing more effective approaches.

The development of learning-based compression methods is much more extended in the computer vision (CV) community. In detail, generative adversarial network (GAN)-based generative compression models [9], [10] have recently gained popularity in CV. GANs are capable of producing visually convincing results that are perceptually similar to the input and thus GAN-based compression displays improved performance in spatial compression even at extremely low bitrates keeping intact the perceptual quality of the reconstructed image. However, the applicability of GANs in spatio-spectral compression of HSIs has not been studied yet.

In this paper, we focus our attention on GANs and explore their effectiveness in achieving lower bitrates with good perceptual reconstruction capability for spatio-spectral compression of HSIs. We select the state-of-the-art high performance GAN-based High Fidelity Compression (HiFiC) [9] as our base model. It consists of blocks with 2D convolutions and thus treats each band separately to perform band-by-band spatial compression. To effectively compress the spectral and spatial information content of HSIs, we introduce two new

Akshara Preethy Byju is with the Department of Computer Science and Engineering, Amrita School of Computing, Amrita Vishwa Vidyapeetham, Amritapuri, India (e-mail: byjuakshara@gmail.com).

Martin Hermann Paul Fuchs and Alisa Walda are with the Faculty of Electrical Engineering and Computer Science, Technische Universität Berlin, Germany (e-mail: m.fuchs@tu-berlin.de; alisa.kore.alice@gmail.com).

Begüm Demir is with the Faculty of Electrical Engineering and Computer Science, Technische Universität Berlin, Germany and also with BIFOLD - Berlin Institute for the Foundations of Learning and Data, Germany (email: demir@tu-berlin.de).

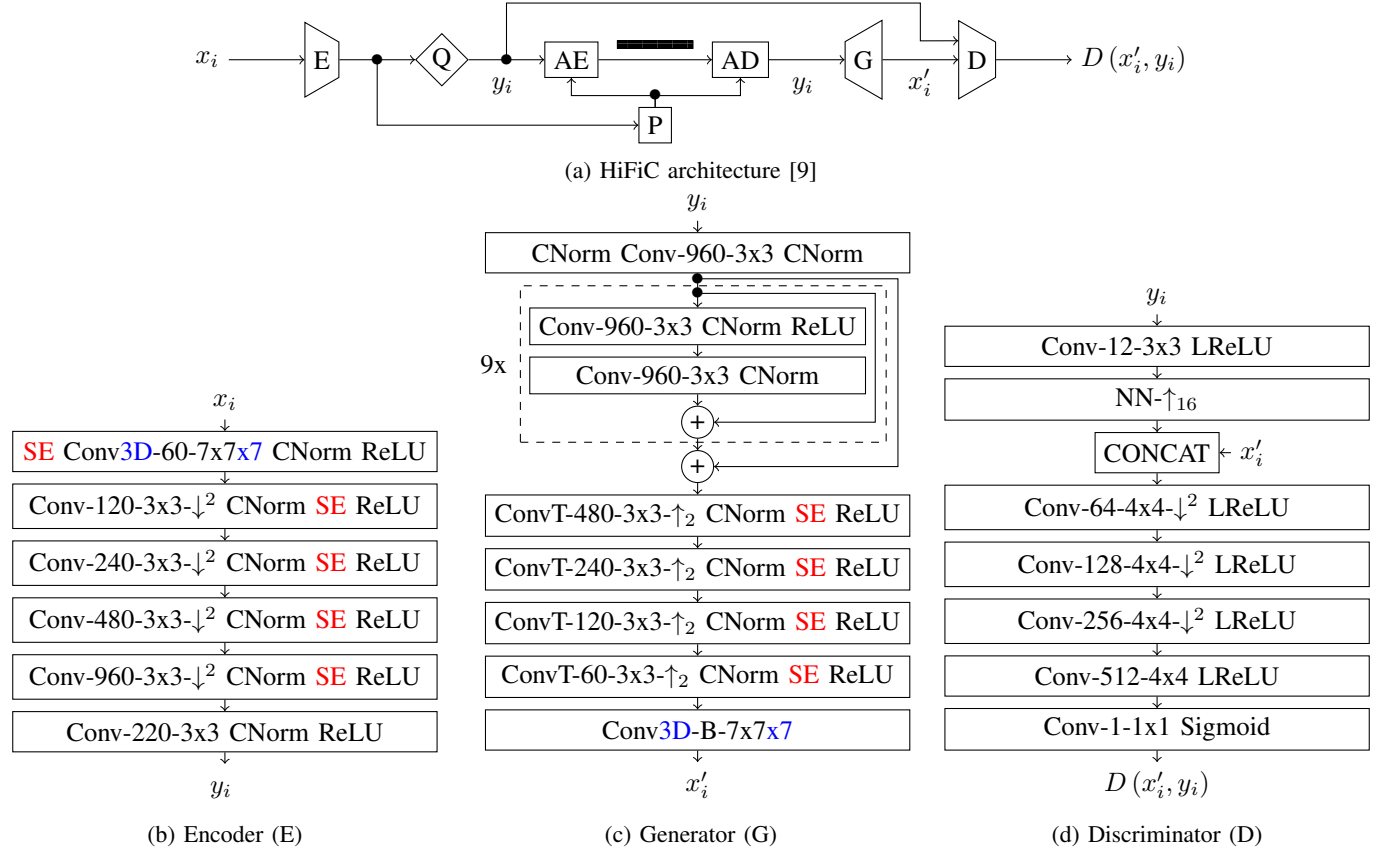


Fig. 1: Proposed spatio-spectral hyperspectral image compression models. (a) The overall GAN-based HiFiC model architecture [9]. (b), (c) and (d) The Encoder (E), Generator (G) and Discriminator (D) architectures of HiFiC_{opt}, HiFiC_{SE} with added SE Blocks and HiFiC_{3D} with two Conv3D layers. Q: quantization, P: probability model, AE: arithmetic encoder, AD: arithmetic decoder, Conv3D(T)-N-KxK(xK): 2D/3D (transposed) convolution layer with N output channels and kernel size K, \downarrow^2/\uparrow_2 : stride 2, CNorm: channel normalization layer, NN- \uparrow_{16} : nearest neighbor upsampling.

models: i) HiFiC_{SE} using squeeze and Excitation (SE) blocks [11]; and ii) HiFiC_{3D} using 3D convolutions (convs) that can exploit both spatial and spectral redundancies. The SE blocks reduce feature redundancies using channel attention while 3D convs use 3D kernels to learn feature dependencies across the channels. Thus, the proposed models are capable of learning to compress spatial and spectral redundancies to achieve better compression performances for HSIs.

II. PROPOSED MODELS FOR SPATIO-SPECTRAL HSI COMPRESSION

Let $\mathbf{X} = \{x_i\}_{i=1}^H$ be a set of H uncompressed HSIs, where x_i is the i^{th} image. The aim of spatio-spectral compression is to produce spatially and spectrally decorrelated latent representations $\mathbf{Y} = \{y_i\}_{i=1}^H$ that can be entropy coded and stored with minimal number of bits. At the same time, the learned representations should retain all the necessary information for reconstructing back $\mathbf{X}' = \{x'_i\}_{i=1}^H$ with the least possible distortion.

The proposed models HiFiC_{SE} and HiFiC_{3D} for the spatio-spectral hyperspectral image compression are defined in the framework of a HiFiC model [9]. Figure 1(a) shows the base HiFiC model with four main blocks: i) encoder E ; ii) probability model P ; iii) generator G ; and iv) discriminator D .

The proposed HiFiC_{SE} and HiFiC_{3D} models follow the base HiFiC but include modifications on the architectures of E and G using SE blocks and 3D convs, respectively (see Figure 1(b) and 1(c)). We introduce these modifications to the architectures to specifically exploit spatio-spectral redundancies. The HiFiC_{SE} consists of SE blocks prior to the regular 2D convs that enable it to attend to the spectral channel information. The SE block consists of layers of global pooling, Fully Connected Multi-Layer Perceptron (FC-MLP) with ReLU activation, where neuron numbers are decreased by reduction ratio r_r , followed by another FC-MLP with Sigmoid activation which outputs weights for each channel (see Figure 2). The SE block investigates the relationship between channels by explicitly modelling the inter-dependencies between them. We use l_1 regularization at the FC-MLP layers for generating sparse weights indicating the channel importance. These weights are then applied to the feature maps to generate the output of the SE block, which can be fed directly into subsequent layers of the network. The HiFiC_{3D} is built by replacing the first 2D conv of the Encoder (E) and the last 2D conv of the Generator (G) with 3D convs where the 3D kernels can evaluate spectral redundancies (see Figure 1(b) and 1(c)). It is inspired from the video compression work in [12] that uses 3D convs to remove temporal redundancies.

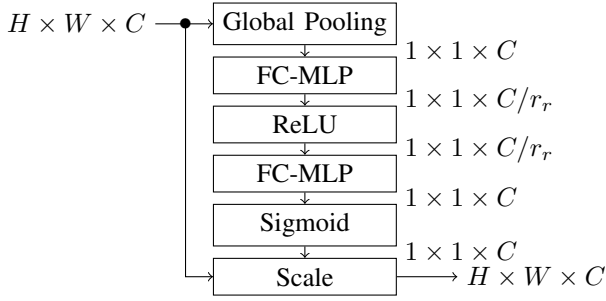


Fig. 2: The basic structure of an SE block [11].

Given an image $x_i \in \mathbf{X}$, it is encoded to a spatially and spectrally decorrelated latent representation y_i and then decoded back to x'_i as:

$$y_i = Q(E(x_i)), x'_i = G(y_i). \quad (1)$$

Where Q is a quantizer which is modeled as rounding operation during inference and straight-through estimator [13] during training. In the bottleneck of the network, the latents y_i are entropy coded into bitstreams using arithmetic encoding (AE) with minimum bitrate $r(y_i) = -\log(P(y_i))$ where P follows the hyper-prior model in [14] with side information. The bitstreams are further decoded back to y_i using arithmetic decoding (AD). Finally, a single-scale discriminator D with the conditional information (y_i) decides if the reconstructed image is real or generated. Each of the modules E , P , G , and D is parameterized by convolutional neural networks and optimized together to obtain the minimum rate-distortion (RD) trade-off. The loss functions L for optimization of each of the four blocks are:

$$L_{E,G,P} = \mathbb{E}_{x_i \sim P_{\mathbf{X}}} [\lambda r(y_i) + d(x_i, x'_i) - \beta \log D(x'_i, y_i)], \quad (2)$$

$$L_D = \mathbb{E}_{x_i \sim P_{\mathbf{X}}} [-\log(1 - D(x'_i, y_i))] + \mathbb{E}_{x_i \sim P_{\mathbf{X}}} [-\log D(x_i, y_i)]. \quad (3)$$

Where $r(y_i)$ is the rate, $d(x_i, x'_i)$ is the distortion loss, λ is the hyperparameter controlling the RD trade-off, and $\log(D(x'_i, y_i))$ is the conditional discriminator loss with β controlling the discriminator loss effect. The distortion loss is modelled as:

$$d(x_i, x'_i) = \theta_1 \cdot \text{MSE} + \theta_2 \cdot (1 - \text{SSIM}) + \theta_3 \cdot \text{LPIPS}. \quad (4)$$

where θ 's are hyperparameters that control the effect of mean square error (MSE), structural similarity index (SSIM), and learned perceptual image patch similarity (LPIPS) losses in the total distortion loss calculation. The LPIPS loss mimics the human visual system and measures reconstruction quality in the feature space, while the SSIM loss is added as an improvement to HSI compression as it enhances reconstruction by preserving the structural information relevant in the scene.

Since $r(y_i)$ is at odds with $d(x_i, x'_i)$ and $-\log(D(x'_i, y_i))$ in (2), controlling the RD trade-off is difficult (as for a fixed λ , different θ 's and β would result in models with different bitrates). Hence, we use target bitrates r_t as in [9] and control λ using $\lambda^{(a)}$ and $\lambda^{(b)}$ with the following rule:

$$\lambda = \begin{cases} \lambda^{(a)}, & \text{if } r(y_i) > r_t. \\ \lambda^{(b)}, & \text{otherwise.} \end{cases} \quad (5)$$

TABLE I: List of target rates r_t 's and its associated $\lambda^{(a)}$ values.

r_t	0.2	0.4	0.6	0.8	1
$\lambda^{(a)}$	2^1	2^0	2^{-1}	2^{-2}	2^{-3}

With $\lambda^{(a)} \gg \lambda^{(b)}$ the model learns bitrates closer to r_t . By keeping $\lambda^{(b)}$ fixed and changing only r_t and $\lambda^{(a)}$, it is possible to achieve different bitrates.

III. DATASET DESCRIPTION AND DESIGN OF EXPERIMENTS

To evaluate the efficacy of our proposed models, we have used a hyperspectral dataset consisting of 3,840 image patches with 369 spectral bands covering the visible and near-infrared (VNIR) portion of the electromagnetic spectrum in the wavelength range between 400 - 1,000 nm. Each patch is a section of 96 x 96 pixels with a spatial resolution of 28cm. We also normalized the data between 0 - 1 which is required for our compression models. The patches are then split in the ratio of 80%, 10% and 10% to form train, validation and test sets, respectively.

All the experiments were carried out in NVIDIA Tesla V100 GPU with 32 GBs of memory. The code for the compression model is implemented with TensorFlow v1.15.2 and build on TensorFlow Compression v1.3 [15] and HiFiC [9]. We trained all the models with Adam optimizer with a batch size of 8. We use a baseline model trained without GAN ($\beta = 0$ in (2)) as an initializer for each of our models. For the distortion loss in (4) we used $\theta_1 = 0.15 \cdot 2^{-5}$, $\theta_2 = 0.075 \cdot 2^{-3}$ and $\theta_3 = 1$. These values were determined through multiple experiments. The discriminator loss effect β was set as 0.15, while the reduction ratio in the SE block r_r was used as 2. As mentioned in Section II, different bitrates can be achieved by changing two hyperparameters: i) target rate r_t ; and ii) $\lambda^{(a)}$. The target rates r_t was varied from [0.2,1] with an interval of 0.2 with its associated $\lambda^{(a)}$ values set accordingly. In total, we configured five settings for each models with different r_t and $\lambda^{(a)}$ combinations (see Table I). We compared the proposed spatio-spectral compression models (HiFiC_{SE} and HiFiC_{3D}) with: i) the adapted (with the loss in (4)) and optimized spatial compression HiFiC model (termed as HiFiC_{opt}); and ii) the traditional JPEG 2000. The comparison was performed at different bitrates and the compression quality was analysed using the reconstruction performance measured using peak signal-to-noise ratio (PSNR) and the compression rate achieved in terms of bitrate measured in bits per pixel (bpp). The higher the PSNR and lower the bpp indicates a better compression performance.

IV. EXPERIMENTAL RESULTS

A. Ablation Study

In this subsection, we present an ablation study to understand the impact of the choice of placement of SE block and 3D conv in HiFiC framework. The performance was evaluated in terms of reconstruction quality measured with average

TABLE II: Performance analysis with placement of SE and 3D Conv Blocks in the HiFiC_{SE} and HiFiC_{3D} models, respectively.

SE block placement	PSNR (in dB)	Runtime (iters/s)
HiFiC _{SE} - E : initial layer	29.80	7.84
HiFiC _{SE} - E : initial+after Norm	30.12	7.49
HiFiC _{SE} - E and G : after Norm	30.89	7.01
HiFiC _{3D} - E and G : all places	30.12	7.31
HiFiC _{3D} - E : initial and G : final	29.24	9.25

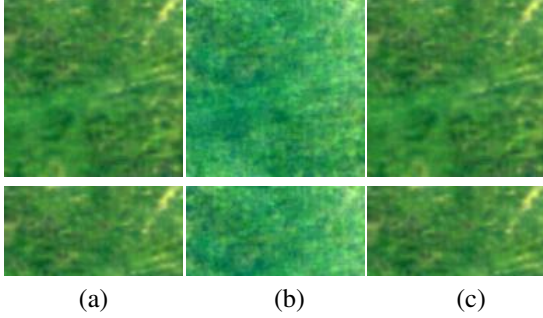


Fig. 3: Impact of the 3D conv layers. (a) Original image, (b) and (c) show reconstructed images without and with 3D convs, respectively. Bottom row: Close-ups of the top image parts.

PSNR and runtime measured as average number of iterations completed per second (iters/s: the higher the value the faster the model) to decide the best placement. The obtained metric by placing the SE and 3D blocks at different layers in the model is provided in Table II. The SE blocks were placed in the initial layer of E alone, then we placed it in the initial layer and after every normalization layer in E , and finally we extended SE blocks to cover all layers in E and G after every normalization layer. We found out that the best PSNR performance with comparable runtime to other placements was achieved when the SE block was incorporated in both E and G after the normalization layer. Similarly, the impact of replacing 2D convs with 3D convs is also analysed.

We found that replacing only the initial layer of E and the final layer of the G works equally well when compared to replacing all 2D convs with an added advantage on the runtime

and computational complexity.

B. Spatio-Spectral HSI Compression

In this subsection, we evaluate the efficacy of our proposed spatio-spectral hyperspectral image compression models. As a first step we analyse the importance of replacing 3D layer in GANs for reconstruction. Fig 3 shows the reconstructed images with HiFiC_{SE} and HiFiC_{3D} using GAN. The reconstruction without 3D conv layer in Figure 3b fails to generate the textures (such as grass) and does not retain visible objects (such as road). But with the integrated 3D conv layer in Figure 3c the perceptual quality is improved and the textures in the grass areas are recovered back. In addition, high quality compressed images are obtained with reduced perceptible artifacts. This shows the importance of the 3D convs in GAN-based models for HSI compression. Figure 4 shows the rate-distortion curves for the spatio-spectral compression methods HiFiC_{SE} and HiFiC_{3D} compared with the optimized spatial compression method HiFiC_{opt} and the traditional JPEG 2000. We can observe that all the end-to-end deep compression methods outperform JPEG 2000 at these small bitrates consistently. Amongst the spatial and spatio-spectral compression methods, we can observe that the HiFiC_{3D} performs slightly better than HiFiC_{SE} and HiFiC_{opt} throughout most bitrates. We observe that the proposed model HiFiC_{3D} achieves significantly higher PSNR values compared to other methods. The qualitative results of reconstruction at $r_t = 0.6$ with the proposed spatio-spectral compression models in comparison with HiFiC_{opt} are also shown in Figure 5. Although the qualitative results look similar with spatial and spatio-spectral compression methods. However, on closer inspection we notice slight improvement in edge details and sharpness which results in better PSNR at lower bpp with the spatio-spectral compression models HiFiC_{SE} and/or HiFiC_{3D} when compared to HiFiC_{opt}.

Improvement in visual quality with increase in bpp is depicted in Figure 6. With increase in the bitrate the reconstruction results obtained improves in visual quality as well as PSNR. The figure also shows that at lower bpp the HiFiC_{3D} in Figure 6 (first row) is better when compared to HiFiC_{SE}. Unlike HiFiC_{SE} that distorts the image appearance with artifacts at lower bpp, HiFiC_{3D} also demonstrates better reconstruction.

V. CONCLUSION

In this paper, we have studied the effectiveness of the generative adversarial networks (GAN)-based models for spatio-spectral compression of hyperspectral images (HSIs). To this end, we have proposed two models: i) HiFiC_{SE} made with Squeeze and Excitation (SE) blocks; and ii) HiFiC_{3D} made with 3D convolutions. Experimental results show that the proposed models remarkably outperform JPEG 2000 by reducing the redundancy in latent representations. In addition, compared to the spatial compression model HiFiC_{opt}, the proposed HiFiC_{SE} and HiFiC_{3D} provide higher PSNR values for the same bitrate producing perceptually better reconstructions with richer details. As a future work, we plan to explore the proposed models in the framework of the scene classification and content-based image retrieval within the 3D compressed

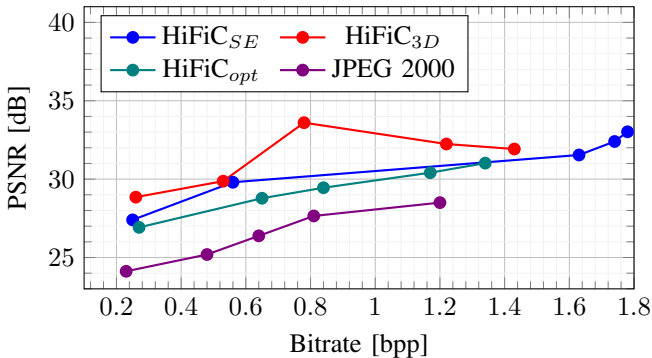


Fig. 4: Rate-distortion performance of our proposed HiFiC_{SE} and HiFiC_{3D} compared to HiFiC_{opt} and JPEG2000.



Fig. 5: (a) Original image. Reconstructed images with (b) HiFiC_{opt}, (c) HiFiC_{SE} and (d) HiFiC_{3D}. The PSNR and achieved bpp are shown below each image as (PSNR, bpp).

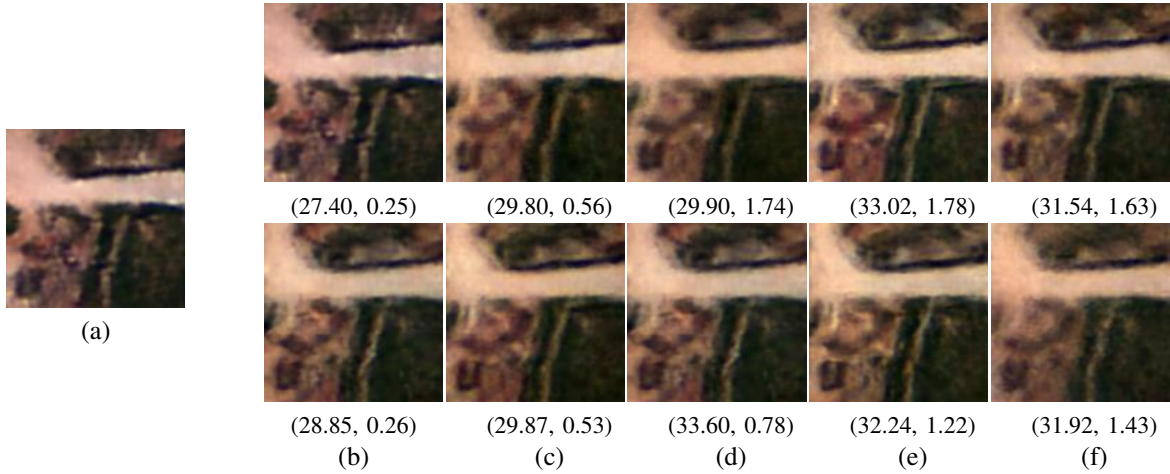


Fig. 6: (a) Original image. Reconstructed results with HiFiC_{SE} (first row) and HiFiC_{3D} (second row) at r_t : (b) 0.2 (c) 0.4 (d) 0.6 (e) 0.8 and (f) 0.1. The PSNR and achieved bpp are shown below each image as (PSNR, bpp).

domain. In addition, we plan to consider strategies that integrate lossless compression only for the particular areas of interest within the HSIs.

ACKNOWLEDGMENT

This work is funded by the European Research Council (ERC) through the ERC-2017-STG BigEarth Project under Grant 759764. The Authors would like to thank Nimisha Thekke Madam for the joint discussions during the initial phase of this study.

REFERENCES

- [1] Q. Du and J. E. Fowler, "Hyperspectral image compression using jpeg2000 and principal component analysis," *IEEE Geoscience and Remote sensing letters*, vol. 4, no. 2, pp. 201–205, 2007.
- [2] M. Rabbani, "Book review: Jpeg2000: Image compression fundamentals, standards and practice," 2002.
- [3] S. Lim, K. Sohn, and C. Lee, "Compression for hyperspectral images using three dimensional wavelet transform," in *IGARSS 2001. Scanning the Present and Resolving the Future. Proceedings. IEEE 2001 International Geoscience and Remote Sensing Symposium (Cat. No. 01CH37217)*, vol. 1. IEEE, 2001, pp. 109–111.
- [4] G. P. Abousleman, M. W. Marcellin, and B. R. Hunt, "Compression of hyperspectral imagery using the 3-d dct and hybrid dpcm/dct," *IEEE transactions on geoscience and remote sensing*, vol. 33, no. 1, pp. 26–34, 1995.
- [5] J. Kuester, W. Gross, and W. Middelmann, "1d-convolutional autoencoder based hyperspectral data compression," *The International Archives of Photogrammetry, Remote Sensing and Spatial Information Sciences*, vol. 43, pp. 15–21, 2021.
- [6] J. Kuester, W. Gross, S. Schreiner, M. Heizmann, and W. Middelmann, "Transferability of convolutional autoencoder model for lossy compression to unknown hyperspectral prisma data," *IEEE Workshop on Hyperspectral Imaging and Signal Processing: Evolution in Remote Sensing (WHISPERS)*, pp. 1–5, 2022.
- [7] R. La Grassa, C. Re, G. Cremonese, and I. Gallo, "Hyperspectral data compression using fully convolutional autoencoder," *Remote Sensing*, vol. 14, no. 10, p. 2472, 2022.
- [8] Y. Chong, L. Chen, and S. Pan, "End-to-end joint spectral-spatial compression and reconstruction of hyperspectral images using a 3d convolutional autoencoder," *Journal of Electronic Imaging*, vol. 30, no. 4, p. 041403, 2021.
- [9] F. Mentzer, G. D. Toderici, M. Tschannen, and E. Agustsson, "High-fidelity generative image compression," *Advances in Neural Information Processing Systems*, vol. 33, 2020.
- [10] L. Wu, K. Huang, and H. Shen, "A gan-based tunable image compression system," in *Proceedings of the IEEE/CVF Winter Conference on Applications of Computer Vision*, 2020, pp. 2334–2342.
- [11] J. Hu, L. Shen, and G. Sun, "Squeeze-and-excitation networks," *arXiv preprint arXiv:1709.01507*, 2017.
- [12] A. Habibian, T. v. Rozendaal, J. M. Tomczak, and T. S. Cohen, "Video compression with rate-distortion autoencoders," in *Proceedings of the IEEE/CVF International Conference on Computer Vision*, 2019, pp. 7033–7042.
- [13] L. Theis, W. Shi, A. Cunningham, and F. Huszar, "Lossy image compression with compressive autoencoders," *arXiv preprint arXiv:1703.00395*, 2017.
- [14] J. Ballé, D. Minnen, S. Singh, S. J. Hwang, and N. Johnston, "Variational image compression with a scale hyperprior," in *International Conference on Learning Representations*, 2018.
- [15] J. Ballé, S. J. Hwang, N. Johnston, D. Minnen, and E. Agustsson, "Tensorflow compression. [Online]. Available: <https://github.com/tensorflow/compression>